THE JOURNAL OF PHYSICAL CHEMISTRY C
A JOURNAL OF THE AMERICAN CHEMICAL SOCIETY

pubs.acs.org/JPCC

Article

Formation of LiF_4TCNQ Complexes During High Concentration Anion-Exchange Doping of Semiconducting Polymers

Published as part of The Journal of Physical Chemistry C special issue "Mark A. Johnson Festschrift".

Zerina Mehmedović, Alex Leon Ruiz, Amanda N. Nguyen, Kara Lo, Diego Garcia Vidales, Xinyu Liu, Charlene Z. Salamat, Evan Doud, Alexander M. Spokoyny, Sarah H. Tolbert, and Benjamin J. Schwartz*

Cite This: *J. Phys. Chem. C* 2025, 129, 15771−15781

Read Online

ACCESS | Metrics & More | Article Recommendations | Supporting Information

ABSTRACT: Anion-exchange doping, in which a semiconducting polymer is exposed to a solution containing both a dopant and an electrolyte, has become a popular method to create polarons on conjugated polymers to increase their electrical conductivity. Although many different initiator dopants can be used, a common dopant/salt combination for anion-exchange *p*-doping is 2,3,5,6-tetrafluoro-tetracyanoquinodimethane (F_4TCNQ) and lithium bis(trifluoromethane) sulfonimide (LiTFSI). Depending on the concentration of initiator dopant, it is usually presumed that all the F_4TCNQ^- ions that remain after doping are exchanged out by mass action for the salt anion, $TFSI^-$. When both LiTFSI and F_4TCNQ are present in excess, however, we find that two new peaks appear in the UV−visible absorption spectrum of anion-exchange-doped conjugated polymers that are not seen when conventionally doping without the addition of salt. We further see that these peaks appear in the same spectral regions, ∼1.95 and ∼3.65 eV, independent of the conjugated polymer being doped by F_4TCNQ/TFSI anion exchange, and that they do not appear when initiator dopants other than F_4TCNQ are used. With the aid of Resonance Raman spectroscopy and quantum chemistry calculations, we assign these peaks to a LiF_4TCNQ complex that forms during the exchange process of anion-exchange doping and remains in the doped polymer film. We estimate that roughly ∼25% of the F_4TCNQ^- ions present during the anion exchange doping process are converted into LiF_4TCNQ complexes, and show that the complex can be dissociated back into F_4TCNQ^- by washing with an appropriate solvent.

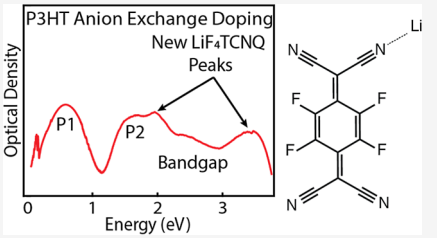

1. INTRODUCTION

Conjugated polymers are a promising class of organic materials for use in electronic devices such as thermoelectrics, solar cells, and organic photovoltaics.[1−6] Although their electrical conductivity is inherently low, their electrical properties can be improved by doping the polymer by either adding (*n*-doping) or removing (*p*-doping) electrons from the conjugated backbone.[7,8] The charge carriers created this way are accompanied by a distortion of the polymer backbone from aromatic to quinoid; the charge, unpaired spin, and structural rearrangement are collectively referred to as a polaron. In order to keep the system electrically neutral, a counterion generated by the doping process is also inserted into the polymer matrix.[7]

Recently, Yamashita et al. developed a new doping technique in which a molecular oxidant (for p-doping) is introduced to the polymer in the presence of a high concentration of inert salt.[9] This method, referred to as anion-exchange (AX) doping, uses mass action to exchange the dopant counterion for a salt anion. AX doping provides the benefits of facile tunability of the choice of counterion as well as increased stability of the doped polymer films. This method also increases the energetic driving force for doping,[9−11] thus improving the electrical conductivity compared to conventional doping methods. Because of these advantages, AX doping has been used to explore the role of counterion size in determining the electrical properties of doped polymer films,[12−14] as well as to quantify the interaction between counterions and environmental factors such as humidity.[15]

AX doping has been studied using multiple different polymers and initiator dopants.[9−11,15−22] A standard combination includes the conjugated polymer poly(3-hexylthiophene-2,5-diyl) (P3HT), the well-studied molecular oxidant 2,3,5,6-tetrafluoro-tetracyanoquinodimethane (F_4TCNQ), and the inert electrolyte lithium bis(trifluoromethane) sulfonimide (LiTFSI), the chemical structures of which all can be found in Figure 1.

Chemical doping of P3HT forms two new electronic states between the polymer's valence band and conduction band. These new states created upon doping lead to three new

Received: April 29, 2025
Revised: July 18, 2025
Accepted: August 1, 2025
Published: August 21, 2025

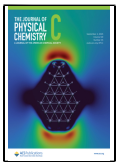

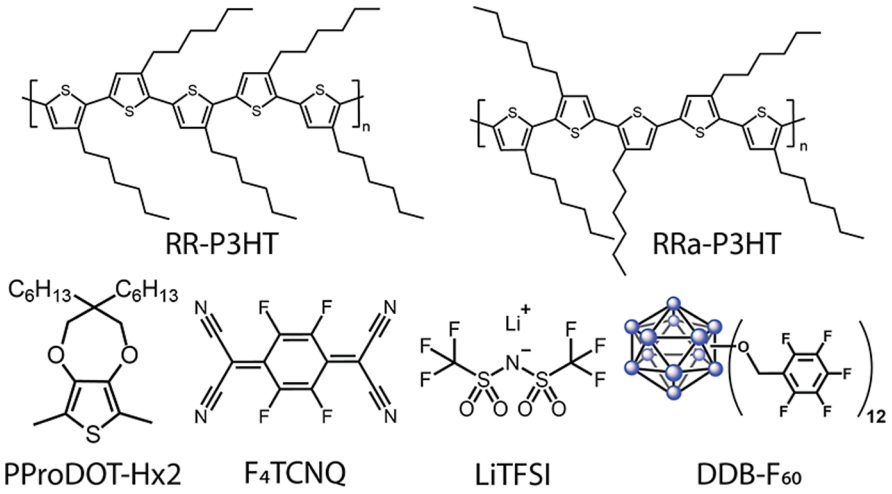

Figure 1. Structures of the various polymer, dopants and salt used in this study. The top row shows the two different structures of P3HT: regioregular (RR) P3HT (top left) and regiorandom (RRa) P3HT (top right). The bottom row, from left to right, shows the structure of a secondary polymer, (PProDOT-Hx_2), the initiator dopant, F_4TCNQ, the LiTFSI electrolyte used for AX doping, and the dopant DDB-F_{60}, where the blue spheres indicate B atoms.

optical transitions associated with the presence of polarons, labeled P1, P2, and P3 on the energy diagram of a doped polymer shown in Figure 2. These transitions can be observed

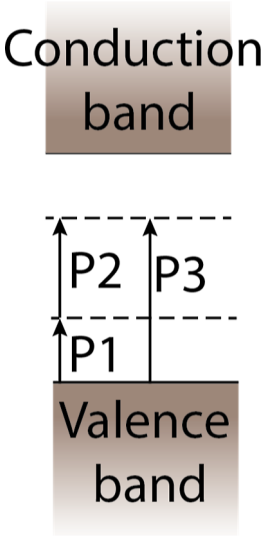

Figure 2. Energy level diagram of a p-doped conjugated polymer with the polaronic optical transitions labeled. The lower midgap state is singly occupied, and the bandgap transition connects the valence and conduction bands (cf. Figure 3).

using UV−vis/NIR spectroscopy, and their presence is often used to confirm doping. For example, when conventionally doping P3HT with F_4TCNQ (as seen below in Figure 3a,b,d,e), the doped polymer (see Experimental Methods for how the films were created) shows both P1 and P2 optical transitions near 0.5 and 1.5 eV, respectively, confirming the formation of polarons. The P3 transition is usually forbidden by symmetry and generally appears only weakly or not at all.[23−27] The F_4TCNQ^- anion also has absorption features at 1.4, 1.6, 1.8, and 3.0 eV, as highlighted on the dashed curves in Figure 3a,b,d,e by asterisks, verifying the presence of the counterion in F_4TCNQ-doped conjugated polymer films.

As previously stated, the AX doping method exchanges out the dopant counterion for the salt anion by mass action. The absence of F_4TCNQ^- anion peaks following AX doping indicates a successful exchange process, as the $TFSI^-$ anion does not absorb in the spectral region shown in Figure 3. The solid traces in Figure 3a,b,d show the spectroscopy of P3HT films that have been AX doped with F_4TCNQ and LiTFSI (again, see the Experimental Methods section for details of the film fabrication), where the disappearance of the F_4TCNQ^- counterion peaks indicate successful counterion exchange.

Although many studies have been published using AX doping,[9−11,15,28,29] the chemistry that takes place during this process involves more than simple mass action ion exchange. For example, in some cases, we see the presence of two new electronic absorption peaks at ∼1.95 and ∼3.65 eV (which we refer to as the Z and Z' peaks, respectively), highlighted in Figures 3a,d,e, that do not appear following conventional doping. As far as we are aware, these absorption features have not been discussed or assigned in the literature, even though they have been observed in at least one other AX doping study independent from our group.[30] The purpose of this paper is to explore these two peaks that are associated with AX doping and determine what new electronic species is created via this process. Throughout what follows, we will consider four different possible assignments for these two peaks, including: (1) a P3 transition that has somehow become less symmetry-forbidden,[31−33] (2) a charge−transfer complex (CTC) between the polymer and initial dopant,[34−38] (3) a dianion of the initial dopant formed via an AX-assisted double-doping process,[39,40] or (4) a LiF_4TCNQ complex formed during the exchange process.[29,41−43] We will consider each of these potential assignments in turn.

The first idea that we will consider is that the new AX-doping spectral feature near 1.95 eV might be the P3 transition (cf. Figure 2). As mentioned above, the P3 transition in doped conjugated polymers is typically symmetry forbidden.[24,44] Based on the energy level diagram in Figure 2, for P3HT, the energy of the P3 transition should be the sum of the energies of the P1 (∼0.5 eV) and P2 (∼1.5 eV) transitions, which is precisely the energy of the observed AX-doping induced spectral feature. Thus, it is possible that the AX

https://doi.org/10.1021/acs.jpcc.5c02950
J. Phys. Chem. C 2025, 129, 15771−15781

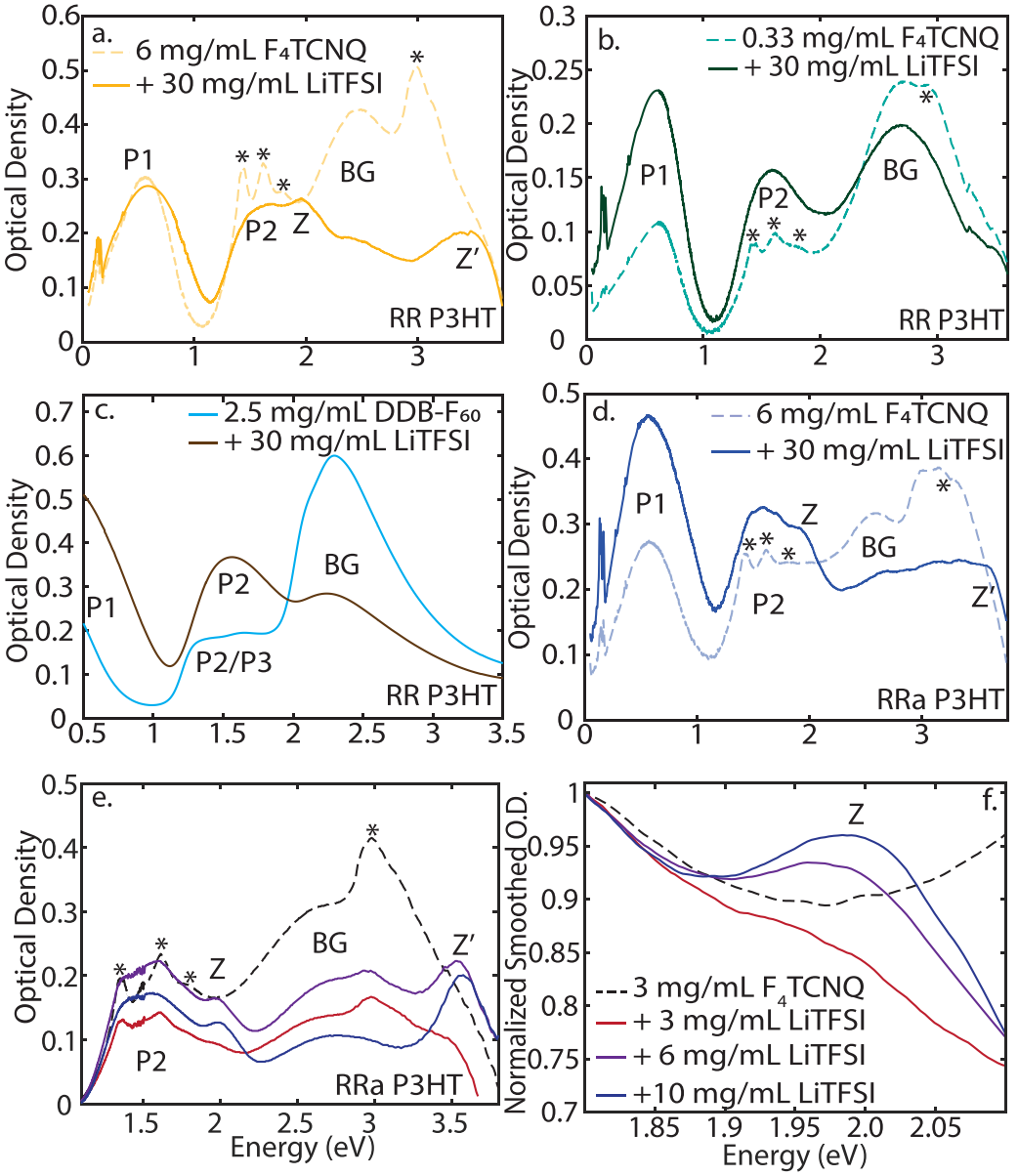

Figure 3. (A) UV−visible−NIR absorption spectra of regioregular (RR) P3HT conventionally doped by sequential processing with a 6 mg mL^{-1} F_4TCNQ in *n*-butyl acetate (*n*-BA) solution (dashed yellow trace) and anion-exchange (AX) doped with a solution of 6 mg mL^{-1} F_4TCNQ and 30 mg mL^{-1} LiTFSI dissolved in *n*-BA (solid yellow trace). The *Z* (1.95 eV) and *Z*′ (3.65 eV) peaks that are the subject of this work, the polaron transition peaks, and the polymer bandgap (BG) transition are labeled; F_4TCNQ^- absorption features are denoted by asterisks. (B) Absorption spectra of RR P3HT conventionally doped with a solution of 0.33 mg mL^{-1} of F_4TCNQ in *n*-BA (dashed teal trace) and AX doped with 0.33 mg mL^{-1} of F_4TCNQ and 30 mg mL^{-1} of LiTFSI (black trace) in *n*-BA. There is no sign of either the *Z* or *Z*′ peaks in the AX doped sample with this low initiator concentration. (C) Absorption spectra of RR P3HT conventionally doped with a 2.5 mg mL^{-1} solution of DDB-F_{60} in *n*-BA, plotted in light blue, and AX doped with a solution of 2.5 mg mL^{-1} DDB-F_{60} and 30 mg mL^{-1} LiTFSI in *n*-BA. There is no sign of the *Z* or *Z*′ peaks when DDB-F_{60} is used as the initiator for AX doping. (D) Absorption spectra of regiorandom (RRa) P3HT conventionally doped with a solution of 6 mg mL^{-1} F_4TCNQ in *n*-BA (dashed blue trace) and AX doped with solution of 6 mg mL^{-1} F_4TCNQ and 30 mg mL^{-1} LiTFSI (solid blue trace) in *n*-BA; the AX doped film clearly shows the *Z* and *Z*′ peaks in the same location as in AX doped RR P3HT films (as do AX doped films of PProDOT-Hx_2, as shown in the SI). (E) Absorption spectra of RR P3HT doped with a solution of 3 mg mL^{-1} F_4TCNQ with 0, 3, 6, and 10 mg mL^{-1} of LiTFSI in *n*-BA, plotted in black, red, purple, and blue, respectively. The shoulder at 3.2 eV is due to excess neutral F_4TCNQ, and the *Z* and *Z*′ peaks are clearly present at higher salt concentrations. (F) Normalized absorption spectra from panel E on an expanded scale, showing that the *Z* peak appears when the initiator dopant and salt are present in $a \geq 1{:}1$ molar ratio. Electrical conductivities of the samples shown in panels a,b,d are given in Table S1 of the Supporting Information.

doping process produces some type of structural change that is drastic enough to disrupt the symmetry and make the P3 transition more strongly allowed.

The second idea we consider is that the new AX doping-induced spectral features result from some type of charge−transfer complex (CTC). Typically, chemical doping results in integer charge transfer, in which an electron is entirely removed from the polymer backbone and transferred to the dopant. There are some extreme conditions, however, that result in placement of the dopant so that electron density is

https://doi.org/10.1021/acs.jpcc.5c02950
J. Phys. Chem. C 2025, 129, 15771−15781

shared between the polymer and the F_4TCNQ; such a species is known as a CTC.[34−38] CTC formation between P3HT and F_4TCNQ is characterized by a broad electronic absorption feature near 2.0 eV, similar to the Z peak we observe with AX doping.[37] P3HT/F_4TCNQ CTCs are also characterized by a C≡N vibrational signature on the partially negatively charged F_4TCNQ at ∼2200 cm^{-1}, and by a broadening of the P1 peak to have significant absorption at 0.65 eV.[37] Although some CTCs are typically always present in F_4TCNQ-doped P3HT films,[34,37] producing a significant amount of CTCs usually requires extreme processing conditions such as high-temperature annealing, using a branched-side-chain polymer to force dopants into the π-stacks, or using solvents that dissolve and recrystallize the doped polymer.[37,45,46] Thus, it is possible that AX doping is another example of an extreme processing condition that encourages the formation of CTCs.

The third plausible assignment for the Z and Z' peaks that we consider is that incorporating LiTFSI into the dopant solution increases the doping potential of F_4TCNQ enough to double dope P3HT. Studies have shown that even though it is an anion, F_4TCNQ^- is capable of oxidizing low ionization energy conjugated polymers.[39] The absorption spectra of $(Li^+)_2F_4TCNQ^{2-}$ shows an electronic feature at 3.7 eV, in the general location where we see the Z' peak.[39] Other work has suggested that F_4TCNQ^{2-} in solution may absorb in the visible region at 481 nm (2.57 eV) or at 567 nm (2.19 eV),[40,47] near where we see the Z peak. Thus, it is possible that the additional oxidation potential obtained through AX doping allows for the removal of two electrons per dopant from the polymer backbone, giving rise to F_4TCNQ^{2-} counterions in the doped films and thus the Z and Z' peaks.

Finally, we consider the idea that the new absorption features arise from a LiF_4TCNQ complex trapped in the AX doped polymer films. Previous studies have explored using F_4TCNQ to dope silver nanoparticles in order to improve their electronic capabilities in devices;[28,29,48−50] one such study suggested that a AgF_4TCNQ complex forms that absorbs at 2.0 eV,[50] precisely where we see the Z peak. These studies thus suggest that forming a cationic complex with F_4TCNQ^- is possible, leading us to consider the LiF_4TCNQ complex as a possible assignment for the Z and Z' peaks. In what follows, we sort through each these four possibilities using a series of experiments and quantum chemistry calculations. We conclude based on the evidence that the new spectral peaks arise from a LiF_4TCNQ complex that forms during the AX doping process and remains behind in the doped polymer film.

2. EXPERIMENTAL METHODS

To study what happens during anion-exchange (AX) doping that produces the Z and Z' absorption peaks, we AX doped three different conjugated polymers: regioregular (RR) and regioregular (RRa) P3HT, and dihexyl-substituted poly(3,4-proylene-dioxythiophene) (PProDOT-Hx_2);[51] see Figure 1 for chemical structures. The chemical doping of all three polymers was performed using sequential processing (SqP), a method developed in our group that produces a superior film quality compared to blend casting.[52,53] SqP entails casting the polymer on a substrate first, followed by a second step casting the dopant from a solvent that is carefully chosen to swell but not dissolve the polymer film. RR P3HT was dissolved at a 2% w/v concentration in 1,2-dichlorobenzene (o-DCB) while RRa P3HT was dissolved in a 1% w/v concentration in chloroform (CF). Following SqP, in the subsequent doping step, the initiator dopant, F_4TCNQ, and for AX doping, the inert salt, LiTFSI, were dissolved in n-butyl acetate (n-BA) with varying concentrations. 100 μL of the dopant solution was allowed to sit on top of the polymer film for 80 s, to allow time for the doping and exchange process to unfold, before the excess solution was spun off. A more detailed description of the experimental procedure, including spin times and concentrations can be found in the Supporting Information. We also performed electrical conductivity measurements of our doped samples (see Table S1 in the Supporting Information) but found that the presence of the Z and Z' peaks do not appear to affect the electrical properties, as discussed in more detail in Section S4 of the Supporting Information.

3. FORMATION CONDITIONS FOR THE Z AND Z' PEAKS

To determine which of these four assignments, if any, makes the most sense for the Z and Z' peaks that appear upon AX doping of conjugated polymers, we first explored whether or not the presence of the peaks depends on the choice of initiator dopant. Both we (see solid traces in Figure 3a,d) and others[30] have seen that the Z and Z' peaks appear when using the common AX dopant/salt combination, F_4TCNQ and LiTFSI. Thus, we used a different initiator dopant to determine if the peaks are associated with the use of F_4TCNQ. Figure 3c shows the absorption spectra of P3HT both conventionally doped with a dodecaborane-based dopant (DDB-F_{60},[45,46] blue curve, see Figure 1 for chemical structure) and AX-doped with DDB-F_{60} and LiTFSI (brown curve). In the conventionally doped sample in this low doping regime, the local symmetry is broken, allowing for the P3 peak to weakly appear.[54] The P3 peak is not observed in the AX-doped sample, which is more strongly doped as evidenced by the higher intensity of both the P1 and P2 peaks and the increased depletion of the bandgap absorption. Most importantly, however, the AX-doped sample shows no signs of either the Z or Z' peaks. This suggests that the electronic species that absorbs at 1.95 and 3.65 eV is associated with the F_4TCNQ dopant.

We note that in their original AX doping study, Yamashita et al. used F_4TCNQ as the initiator dopant and 1-ethyl-3-methylimidazolium bis(trifluoromethylsulfonyl)imide (EMIM-TFSI) as the salt.[9] When these workers used the same concentrations of dopant and salt as we used in Figure 3a, they did not observe any sign of the Z or Z' peaks.[9] This is also consistent with the idea that the combination of F_4TCNQ and LiTFSI is essential in forming the new absorbing electronic species.

Since it appears that the F_4TCNQ/LiTFSI dopant/salt combination is necessary to create the Z and Z' peaks following AX doping, we turn next to see if formation of the species responsible for these peaks depends on the concentration of either the dopant or the salt. We first limited the dopant concentration (0.33 mg mL^{-1} or 1.2 mM F_4TCNQ) while keeping the salt in excess (30 mg mL^{-1} or 105 mM LiTFSI); the spectra of the resulting AX-doped P3HT films are shown in Figure 3b. The conventionally doped sample (dashed teal trace) verifies that the polymer is indeed doped with F_4TCNQ, as confirmed by the presence of F_4TCNQ^- anion absorption peaks, highlighted with asterisks. The AX-doped sample (solid green trace) shows that the exchange process was successful because the F_4TCNQ^- peaks disappear upon the addition of excess LiTFSI. In this dopant-

https://doi.org/10.1021/acs.jpcc.5c02950
J. Phys. Chem. C 2025, 129, 15771−15781

limited case, however, we see no signs of the Z and Z' peaks, indicating that there are specific concentration conditions for formation of the species responsible for these peaks.

We next tested the AX salt content to help understand the conditions under which the new species begins to form. Figure 3e shows the absorption spectra of P3HT doped with 3 mg mL^{-1} (10.9 mM) F_4TCNQ, and AX-doped with the addition of 3, 6, or 10 mg mL^{-1} (10.5, 20.9, and 34.8 mM, respectively) of LiTFSI. Figure 3f shows a zoom-in of the Z-peak region near 2 eV, with the spectra normalized at 1.8 eV for ease of comparison. When the dopant to salt ratio is less than 1:1 (black and red traces), F_4TCNQ^- anion peaks are still visible. This indicates that equimolar ratios of salt must be present to fully exchange out all of the original dopant counterions. More importantly, only when the salt is in molar excess (purple and blue traces) are the Z (and Z') peaks formed. This indicates that formation of the species that absorbs at 1.95 and 3.65 eV is contingent on having an excess concentration of both dopant and salt. Therefore, for the remainder of this study, we focus on doping P3HT with 6 mg mL^{-1} (21.7 mM) F_4TCNQ and 30 mg mL^{-1} (104.5 mM) LiTFSI, as in Figure 3a,d, to better understand the species responsible for the Z and Z' absorption peaks that is readily made under this doping condition.

4. THE Z AND Z' PEAKS APPEAR IN THE SAME LOCATION WITH DIFFERENT POLYMERS

Now that we have established that the peaks have specific formation conditions, we can use a combination of experimental and theoretical studies to explore the four possible assignments. First, the idea that the Z peak at 1.95 eV could be a broken symmetry-allowed P3 transition is not consistent with the fact that the Z peak also appears concomitantly with Z' at 3.65 eV. A second reason that the Z peak is likely not the P3 transition comes from the fact that we studied two different P3HT samples with different regioregularities. Regiorandom (RRa) P3HT has a bandgap that is ~0.5 eV bluer than the regioregular (RR) P3HT that we studied in Figure 3a−c,e. When doped, RRa P3HT has its P1 transition at 0.65 eV and its P2 transition at 1.65 eV (see dashed trace Figure 3d), suggesting that the P3 transition should occur near 2.3 eV. However, AX doping of RRa P3HT (Figure 3d) with the same 6 mg mL^{-1} F_4TCNQ 30 mg mL^{-1} LiTFSI solution that we used for RR P3HT (Figure 3a) shows that the Z and Z' peaks are in the exact same spectral positions. Furthermore, in Figure S2 in the Supporting Information, we compare conventional and AX doping of PProDOT-Hx_2 and again find that the Z and Z' peaks are in the exact same location. All of these results indicate that these peaks are not associated with the P3 transition of the doped polymer.

5. FTIR SPECTROSCOPY OF ANION-EXCHANGE-DOPED P3HT

Since it appears that F_4TCNQ is necessary to create the species responsible for the Z and Z' peaks, we can take advantage of the fact that the vibrational stretching modes of the nitrile groups on the F_4TCNQ dopant absorb in an otherwise spectrally quiet region to probe what is happening with FTIR spectroscopy. It is well-known that the B_{1u} and B_{2u} vibrational modes of F_4TCNQ^-, which are generally located at ~2190 cm^{-1} and ~2170 cm^{-1}, respectively, shift depending on the charge on the molecule as well as the degree of polaron localization and crystallinity of the nearby doped polymer.[55]

Figure 4a,b show the normalized C≡N stretching vibrations for both conventionally- and AX-doped samples of RR and RRa P3HT, respectively. The conventionally doped samples (dashed traces) have their F_4TCNQ^- B_{1u} and B_{2u} modes at 2188 and 2170 cm^{-1} in RR P3HT, and at 2190 and 2166 cm^{-1} in RRa P3HT. The AX-doped samples (solid traces), however, show nitrile stretching peaks at ~2200 and ~2220 cm^{-1} for both RR and RRa P3HT, even though there is no sign of the electronic absorption of F_4TCNQ^- in these samples. We also note that these frequencies are too high to be associated with F_4TCNQ^-, but given the spectral region, they must be nitrile stretches on some form of F_4TCNQ that has remained in the AX-doped films.

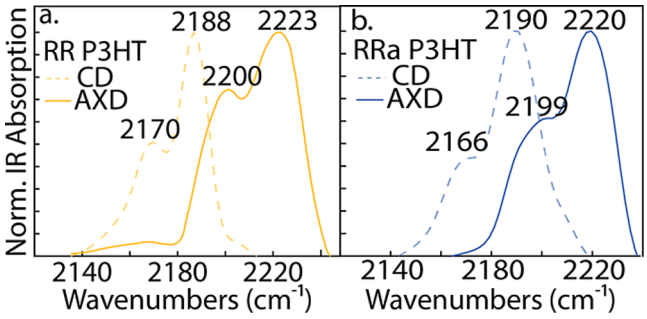

Figure 4. F_4TCNQ nitrile stretch FTIR vibrational spectra for (a) RR and (b) RRa P3HT conventionally doped (CD) with 6 mg mL^{-1} F_4TCNQ (dashed traces) and anion-exchange doped (AXD) with 6 mg mL^{-1} F_4TCNQ and 30 mg mL^{-1} LiTFSI (solid traces). Both CD samples show the B_{1u} (~2190 cm^{-1}) and B_{2u} (~2170 cm^{-1}) vibrational modes associated with F_4TCNQ^-. The AXD samples for both polymers show a peak close to where P3HT/F_4TCNQ CTCs are known to absorb (2200 cm^{-1}), but they also show a peak near 2220 cm^{-1}, closer to where neutral F_4TCNQ absorbs.

The presence of higher-frequency nitrile stretches on F_4TCNQ in Figure 4, along with the positions of the Z and Z' peaks in Figure 3a,d, appears to suggest the possibility of CTC formation. Indeed, it has been demonstrated that one feature of the CTC that forms between P3HT and F_4TCNQ is the presence of a C≡N stretching mode at 2200 cm^{-1},[34,37] similar to what is seen in Figure 4. CTCs also have been reported to absorb near 2 eV,[37] but the CTC electronic absorption peak is much broader than that observed in Figure 3a,d, and there is no evidence that CTCs absorb near 3.5 eV where we see the Z' peak. Moreover, we do not see any broadening of the P1 peak in Figure 3a,d, another key feature associated with CTC formation in this system.[37] In addition, there are no reports of CTCs with F_4TCNQ having a vibrational absorption at ~2220 cm^{-1} (closer to where neutral F_4TCNQ absorbs), which we also observe in Figure 4. Thus, while we may possibly have created some CTCs upon AX doping of RR and RRa P3HT, it does not appear that the Z and Z' peaks are associated with CTC formation.

6. RESONANCE RAMAN SPECTROSCOPY OF THE F_4TCNQ^- AND Z PEAKS OF CONVENTIONALLY- AND AX-DOPED P3HT

Since it appears that the species giving rise to the Z and Z' peaks is connected to an F_4TCNQ species with shifted vibrations, we turn next to resonance Raman spectroscopy to correlate the electronic transitions with specific nitrile vibrational modes. To accomplish this, we first use 785 nm

https://doi.org/10.1021/acs.jpcc.5c02950
J. Phys. Chem. C 2025, 129, 15771−15781

(1.58 eV) excitation on both conventionally- and AX-doped samples of both RR (Figure 5a) and RRa (Figure 5b) P3HT.

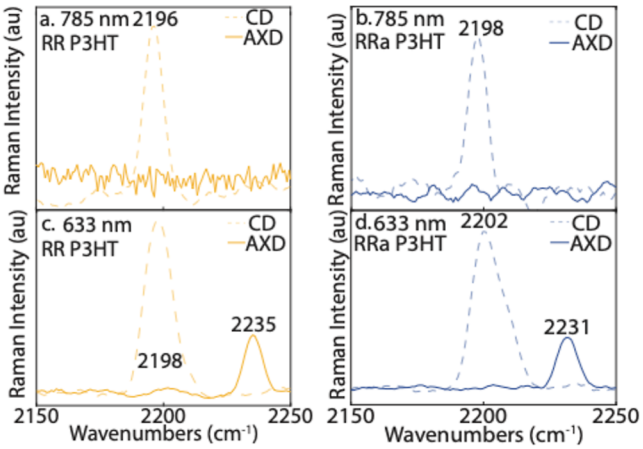

Figure 5. 785 nm excitation resonance Raman spectroscopy of (a) RR and (b) RRa P3HT conventionally doped (CD) with 6 mg mL^{-1} F_4TCNQ (dashed traces) and anion-exchange doped (AXD) with 6 mg mL^{-1} F_4TCNQ and 30 mg mL^{-1} LiTFSI (solid traces). This excitation wavelength is on resonance with the F_4TCNQ^- anion. The CD samples show nitrile stretches at 2196 cm^{-1} and 2198 cm^{-1} for RR and RRa P3HT, respectively. The AXD samples show no detectable nitrile stretches, indicating successful counterion exchange. 633 nm excitation resonance Raman spectroscopy of CD (dashed traces) and AXD (solid traces) (c) RR and (d) RRa P3HT. This excitation wavelength excites the *Z* peak directly. In the CD samples both the RR and RRa P3HT have peaks at ~2200 cm^{-1}, which could correspond to a CTC. The AXD films also have a C≡N stretch that is shifted to 2235 and 2231 cm^{-1} for RR and RRa P3HT, respectively, confirming that the *Z* peak is associated with some F_4TCNQ-related species.

Light at 785 nm is on resonance with the F_4TCNQ^- electronic absorption, which means that we expect to see C≡N stretching vibrations in the resonance Raman spectra of the conventionally doped samples but not in the AX-doped films where most of the counterions have been exchanged away for $TFSI^-$. Indeed, the 785 nm Resonance Raman data shows a nitrile stretching mode only for the conventionally doped samples (dashed traces), with no sign of C≡N stretches in the AX-doped (solid traces) samples. This verifies that the exchange process was successful and that there is not a significant amount of F_4TCNQ^- left in the AX-doped films, reinforcing our conclusion that the *Z* peak is not associated with the bare F_4TCNQ^- anion.

We next turn to on-resonance Raman spectroscopy by exciting the *Z* peak directly at 633 nm (1.96 eV), with the data shown in Figure 5c,d for doped RR and RRa P3HT, respectively. The conventionally doped samples, shown with dashed traces, display peaks at 2198 cm^{-1} and 2202 cm^{-1} for the two polymer environments, which could be consistent with the presence of a CTC between the F_4TCNQ dopant and the host polymer. It is known that the F_4TCNQ/P3HT CTC absorbs at this excitation wavelength, so it would make sense that we could be probing some of the small number of CTCs that are always formed with this dopant, even if they are not strongly evident in the UV-vis-NIR absorption spectrum.[34,37] More importantly, the fact that we see vibrational features around 2198 cm^{-1} when exciting the conventionally doped samples using both 785 and 633 nm wavelengths indicates that the species giving rise to this peak is likely not the same one that forms the *Z* peak. In contrast, when excited at 633 cm^{-1}, the AX-doped films show C≡N vibrational modes at higher wavenumbers, 2235 and 2231 cm^{-1} for RR and RRa P3HT, respectively. Thus, these peaks are indeed associated with nitrile stretches on the F_4TCNQ dopant, but they are not coming from a F_4TCNQ/P3HT CTC.

The position of the vibrational peaks associated with resonant excitation of the *Z* peak also allows us to comment on the possibility of forming an F_4TCNQ^{2-} dianion of the initiator dopant during AX doping of P3HT films. As mentioned in the introduction, there have been literature reports that the F_4TCNQ^{2-} dianion might have an electronic absorption in the visible region of the spectrum near where the *Z* peak absorbs, as well as an absorption at the position of the *Z*′ peak.[39,40,47] However, the F_4TCNQ^{2-} dianion has nitrile vibrational frequencies at 2166 cm^{-1} and 2136 cm^{-1}.[39,40,47] The data in Figures 5c,d show that the C≡N vibrational frequencies associated with the *Z*-peak are nearly 100 wavenumbers blue-shifted from the known F_4TCNQ^{2-} modes. This indicates that the AX process is not conducive to double doping with the P3HT/F_4TCNQ materials combination and that the *Z* and *Z*′ peaks are not associated with F_4TCNQ^{2-}.[39,40,47]

7. QUANTUM CHEMISTRY CALCULATIONS OF DIFFERENT F_4TCNQ-BASED SPECIES

Given that the vibrations of the F_4TCNQ-based species responsible for the *Z* and *Z*′ peaks lie to higher frequency than those of the monoanion, this suggests that the species responsible for these peaks has more of the character of neutral F_4TCNQ. This idea led us to investigate the possibility of having a lithium ion from the electrolyte form a complex with F_4TCNQ^- during the AX doping process; forming such a complex would render the F_4TCNQ^- anion insoluble, potentially leaving it in the doped film. Previous studies using F_4TCNQ to dope Ag nanoparticles suggest that AgF_4TCNQ complexes can form and that they have an electronic absorption near 2 eV.[50] This indicates not only that F_4TCNQ can form complexes with small cations, but also that such complexes could have electronic transitions where we see the *Z* and/or *Z*′ peaks.[50] This idea would also be consistent with the facts that we see these features only when there is a sufficiently high salt and F_4TCNQ concentration, that the peaks are independent of the polymer being doped, and that the peaks do not appear when salts with other cations are used.[9]

To investigate this possibility, we started by performing density functional theory (DFT) quantum chemistry calculations on LiF_4TCNQ complexes with multiple locations of the Li^+ in relation to F_4TCNQ. The calculations are performed at the B3LYP/6-311++G level of theory, with the electronic spectra calculated using TD-DFT, as discussed in more detail in the Supporting Information. Here, we focus on the configuration in which the Li^+ is placed "in line" with one of the cyano groups of F_4TCNQ^-; a cartoon of this geometry is shown in the inset of Figure 6b as well as in the TOC graphic. The calculated vibrational frequencies and ground-state absorption electronic absorption spectrum of LiF_4TCNQ are plotted in Figure 6a,b, respectively. The calculated IR frequencies of F_4TCNQ^- complexed with Li^+ (2239 cm^{-1}) are blue-shifted from those of uncomplexed F_4TCNQ^-, similar to what is seen in the resonance Raman experiments when

https://doi.org/10.1021/acs.jpcc.5c02950
J. Phys. Chem. C 2025, 129, 15771−15781

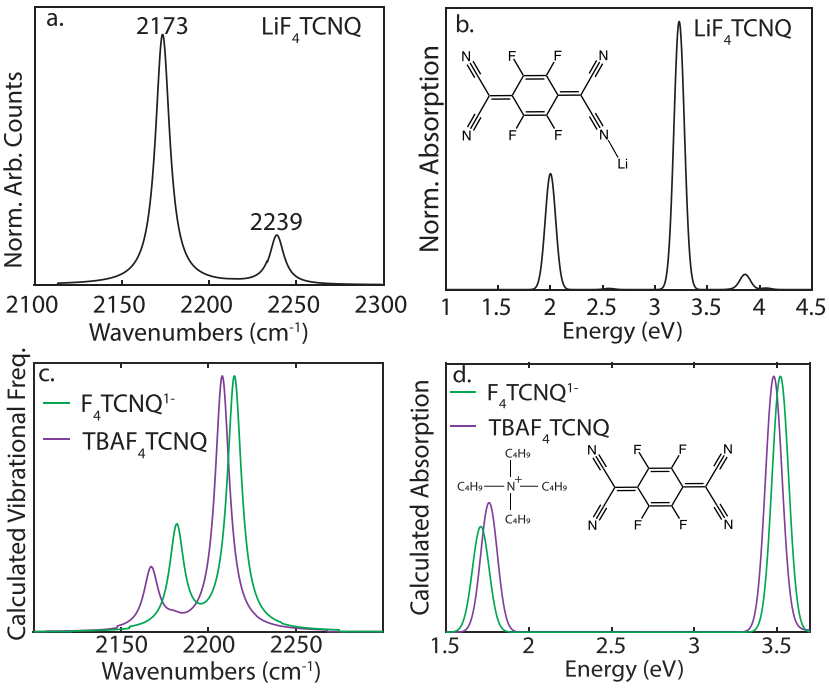

Figure 6. Panels a and b show DFT-calculated vibrational frequencies (IR spectrum) and TD-DFT-calculated electronic absorption of LiF_4TCNQ, respectively. The calculated IR spectrum of the complex shows that the nitrile stretching vibration is significantly blue-shifted compared to that of both the uncomplexed F_4TCNQ^- anion (green curve, panel c) and the F_4TCNQ^{2-} dianion (see the Supporting Information). The absorption spectrum of the LiF_4TCNQ complex shows peaks at 2 and 3.2 eV. Panels c and d show the calculated vibrational frequencies and electronic spectrum of F_4TCNQ^{1-} (green curves) and tetrabutylammonium (TBA)-F_4TCNQ (purple curves), indicating that the large counterion does not affect the electronic structure or vibrational frequencies of F_4TCNQ^- the way that the small Li^+ cation does.

exciting the Z peak on resonance. The calculated electronic absorption for LiF_4TCNQ has peaks at ∼2.0 and ∼3.2 eV, in excellent agreement with the positions of the Z and Z' peaks seen in experiment. Thus, we propose that the Z and Z' peaks seen upon anion-exchange doping of conjugated polymers at high concentrations are associated with a LiF_4TCNQ complex.

We also calculated the properties of F_4TCNQ^- complexed with a tetrabutylammonium (TBA^+) cation, as shown in Figure 6c,d, to test if any positively charged ion could form a species that would give rise to the Z and Z' peaks. The data make clear that unlike with Li^+, the TBA^+ ion does not greatly affect either the vibrations or the electronic absorption of F_4TCNQ^-. This is due to the TBA^+ counterion's size, which places its charge too far away from the F_4TCNQ^- anion to affect its electronic structure, whereas the smaller and higher charge density Li^+ has a much stronger interaction. Thus, different initiator dopant and cation complexes do not form peaks in the visible or shift the nitrile stretches to higher frequencies the way we see experimentally and the way that is predicted for the LiF_4TCNQ complex. Overall, all of the data and calculations support the assignment of the Z and Z' absorption peaks seen following AX doping of conjugated polymers to a LiF_4TCNQ complex that forms after $TFSI^-$ exchanges with F_4TCNQ^-, with the insoluble complex remaining in the doped polymer film.

8. VERIFYING AND QUANTIFYING LIF_4TCNQ COMPLEX FORMATION IN AX DOPING

With our conclusion that the Z and Z' peaks arise from a low-solubility LiF_4TCNQ complex that forms during the AX process and remains trapped in the doped polymer film, we turn next to a brief series of experiments that help verify the assignment of these peaks, and then work to quantify the amount of complex that is formed.

First, we structurally analyzed the AX-doped films using Grazing Incidence Wide Angle X-ray Scattering (GIWAXS), with the results shown in Figure S1 of the Supporting Information. The anion exchange process is known to change the structure of doped P3HT films, both because of the enhanced doping level and because the $TFSI^-$ ion fills space in the P3HT crystal lattice differently than the F_4TCNQ^- anion.[9−11] We find that we see the structural changes expected with AX doping whether or not the Z and Z' peaks are present, indicating that the formation of the complex does not significantly affect the structure of the doped polymer film. However, we do see a small scattering peak at ∼0.56 $Å^{-1}$ whose amplitude roughly scales with the amplitude of the Z and Z' peaks in the absorption spectrum. We speculate that this peak may correspond to the lattice spacing of crystallites of LiF_4TCNQ complexes, a possibility that is discussed in more detail in the Supporting Information.

As a second approach to verify the identity of the Z and Z' peaks as arising from LiF_4TCNQ, we attempted to make the complex electrochemically by reducing F_4TCNQ in solution in the presence of either a LiTFSI or a TBA^+ $TSFI^-$ electrolyte and then casting the reduced solution onto a poly(vinyl alcohol) film. Figure S7 in the Supporting Information shows the results, where the Z and Z' peaks (along with both F_4TCNQ^- and F_4TCNQ absorption bands) are clearly evident when the LiTFSI electrolyte is used, but absent when the TBA^+ $TFSI^-$ electrolyte is used, providing strong verification of our assignment of these peaks to LiF_4TCNQ.

Third, we worked to see if we could 'reverse anion exchange' the LiF_4TCNQ complex by applying a postdoping solvent

https://doi.org/10.1021/acs.jpcc.5c02950
J. Phys. Chem. C 2025, 129, 15771−15781

washing step to break up the complex and regenerate F_4TCNQ^-. To do this, we took a RR P3HT film AX-doped with 6 mg mL^{-1} F_4TCNQ and 30 mg mL^{-1} LiTFSI that displayed the Z and Z' peaks and washed it with pure n-BA. We chose n-BA because the complex should be insoluble in this solvent (given that the complex forms when using this solvent and then remains in or on the doped polymer film). The $TFSI^-$ anion in the doped film, however, is highly soluble in n-BA, so if washing removes $TFSI^-$, this would create a mass action driving force to break up the LiF_4TCNQ complex, using F_4TCNQ^- liberated from the complex to serve as the polaron counterion and releasing Li^+ and $TFSI^-$ into solution.

Figure 7 shows the results of this 'reverse anion exchange' washing experiment; the red trace shows the absorption

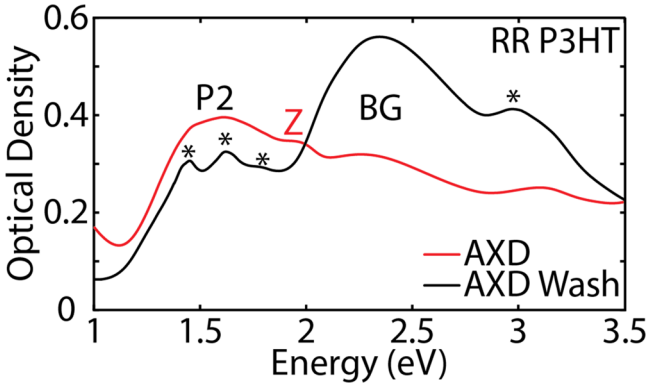

Figure 7. UV−vis−NIR absorption spectra of 97% RR P3HT anion-exchange doped (AXD) with 6 mg/mL F_4TCNQ and 30 mg/mL LiTFSI (same as in Figure 3a) both before (red curve) and after (black curve) washing with n-BA solvent. It is clear that washing the samples removes the Z and Z' peaks that arise from the LiF_4TNCQ by breaking up complex, causing "reverse anion exchange", as evidenced by the appearance of F_4TCNQ^- peaks, which are marked with asterisks. The increase in the BG absorption and decrease in the P2 absorption indicate that the washing process also has partly dedoped the sample.

spectrum of the as-prepared AX-doped P3HT film, while the black trace shows the same film after washing with n-BA. The results show clearly that washing not only eliminates the Z and Z' peaks, but also creates a new population of F_4TCNQ^- (peaks highlighted by asterisks), which could only have come from dissociation of the LiF_4TCNQ complex. Thus, this experiment provides further evidence that the Z and Z' peaks arise from LiF_4TCNQ.

One interesting feature of the spectra in Figure 7 is that the magnitude of the newly formed F_4TCNQ^- peaks following n-BA washing is about ∼25% of that observed following conventional doping with F_4TCNQ (cf. Figure 3a). This suggests that a significant fraction of the F_4TCNQ used in the AX doping process gets tied up in LiF_4TCNQ complexes and remains in the film, leading to the question of the formation yield of the complex. We tried several approaches to quantify the amount of LiF_4TCNQ complex in our AX-doped films. First, we used the calculated oscillator strength of the complex' Z-peak from Figure 6b and the measured optical density of that peak in the AX-doped RRa P3HT sample in Figure 3d (see the Supporting Information for details) to estimate the number density of complexes in that sample. With this analysis, described further in the Supporting Information, we obtained a value of about 1.27×10^{20} absorbers per cm^3. Given that films of P3HT that have been anion-exchanged-doped to a high level have been reported to have a doping density of approximately 4.7×10^{20} cm^{-3},[55] this suggests that ∼25% of the F_4TCNQ molecules used in the initial doping process end up trapped as LiF_4TCNQ complexes after the exchange process is complete.

As a second way to quantify the amount of complex formed during AX doping, we used the amplitude of the ∼2220 cm^{-1} nitrile stretching vibration of the complex in seen in the solid curve in Figure 4b to estimate the amount of complex in the sample. The idea is to compare the amplitude of that peak to the amplitude of the ∼2190 cm^{-1} B_{1u} stretch of F_4TCNQ^- in the conventionally doped sample (dashed curve in Figure 4b), assuming that the IR cross sections of these two peaks are similar. We did this by fitting all of the peaks in the nitrile stretch region, with the unnormalized IR spectral data and fits summarized in Figure S5 and Table S3 in the Supporting Information. We find that the amplitude of nitrile stretch of the LiF_4TCNQ complex is ∼20% that of the B_{1u} peak in the conventionally doped sample, again suggesting that ∼20% of the F_4TCNQ^- anions are trapped by Li^+ and become complexes during the AX doping process.

Finally, we performed X-ray photoelectron spectroscopy (XPS) on a RR P3HT AX-doped sample whose absorption spectra show the Z and Z' peaks (same doping conditions as in Figure 3a). The results are shown in Figure S6 and Table S4 of the Supporting Information. By examining the ratios of the elements Li, F, N and S in the sample, we are able to determine the amount of LiF_4TCNQ complex relative to the amount of $TFSI^-$ that serves as the counterion for the polarons. Of course, XPS primarily probes only the top few nm of the film, whose composition may or may not be representative of the bulk of the film; however, we were able to estimate that about 25% of the F_4TCNQ that is in the film is converted to LiF_4TCNQ, which is similar to the values we obtained from the other analysis methods presented above.

9. CONCLUSIONS

In summary, using UV−visible and FTIR absorption spectroscopy, resonance Raman spectroscopy and density functional theory calculations, we have investigated the origin of the 1.95 and 3.65 eV absorption peaks that appear following high-concentration anion-exchange doping of conjugated polymers. We were able to eliminate possible assignments as arising from the P3 transition of the doped polymer, a CTC between the polymer and the dopant, and dianions of the dopant, but found strong evidence that the species involved is a LiF_4TCNQ complex. When high concentrations of both the dopant and Li^+ are present, there is enough of this complex species to be seen readily seen spectroscopically, indicating that this is an important byproduct of the AX doping process. We were able to estimate using multiple methods that ∼25% of the F_4TCNQ^- anions created upon doping the film become trapped as LiF_4TCNQ complexes during the AX process. We also showed that under the proper conditions, the complex could be dissociated in a 'reverse anion exchange' process, regenerating the original F_4TCNQ^-. The results also extend our understanding of TCNQ-based ionic complexes, which have a rich and varied history in the literature.[40,47]

■ ASSOCIATED CONTENT

Supporting Information

The Supporting Information is available free of charge at https://pubs.acs.org/doi/10.1021/acs.jpcc.5c02950.

https://doi.org/10.1021/acs.jpcc.5c02950
J. Phys. Chem. C 2025, 129, 15771−15781

Readers can find the following information: the specific materials used; film preparation and polymer doping procedures; details about characterization methods such as UV−vis, FTIR, and Raman; conductivity measurements; structural analysis; secondary polymer studies; details about the quantum chemistry calculations; quantitative analysis of the complex; and electrochemical experiments (PDF)

AUTHOR INFORMATION

Corresponding Author

Benjamin J. Schwartz − *Department of Chemistry and Biochemistry, University of California, Los Angeles, California 90095-1569, United States;* orcid.org/0000-0003-3257-9152; Phone: (310)206-4113; Email: schwartz@chem.ucla.edu

Authors

Zerina Mehmedović − *Department of Chemistry and Biochemistry, University of California, Los Angeles, California 90095-1569, United States*

Alex Leon Ruiz − *Department of Chemistry and Biochemistry, University of California, Los Angeles, California 90095-1569, United States*

Amanda N. Nguyen − *Department of Chemistry and Biochemistry, University of California, Los Angeles, California 90095-1569, United States*

Kara Lo − *Department of Chemistry and Biochemistry, University of California, Los Angeles, California 90095-1569, United States*

Diego Garcia Vidales − *Department of Chemistry and Biochemistry, University of California, Los Angeles, California 90095-1569, United States*

Xinyu Liu − *Department of Chemistry and Biochemistry, University of California, Los Angeles, California 90095-1569, United States;* orcid.org/0000-0003-4978-9893

Charlene Z. Salamat − *Department of Chemistry and Biochemistry, University of California, Los Angeles, California 90095-1569, United States;* orcid.org/0000-0001-5581-5029

Evan Doud − *Department of Chemistry and Biochemistry, University of California, Los Angeles, California 90095-1569, United States;* orcid.org/0000-0003-4561-4105

Alexander M. Spokoyny − *Department of Chemistry and Biochemistry, University of California, Los Angeles, California 90095-1569, United States;* orcid.org/0000-0002-5683-6240

Sarah H. Tolbert − *Department of Chemistry and Biochemistry, University of California, Los Angeles, California 90095-1569, United States; Department of Materials Science and Engineering, University of California, Los Angeles, California 90095, United States;* orcid.org/0000-0001-9969-1582

Complete contact information is available at: https://pubs.acs.org/10.1021/acs.jpcc.5c02950

Notes

The authors declare no competing financial interest.

ACKNOWLEDGMENTS

This work was supported by the National Science Foundation under grants CHE-2305152 and DMR-2513790. A.M.S. thanks the Dreyfus Foundation for a Camille Dreyfus Teacher-Scholar Award. Z.M. would like to thank Serigey Prihodko and Boxuan Zhao for their help with the Resonance Raman measurements. The authors would also like to thank one of the referees for suggesting the postprocessing washing experiment.

REFERENCES

(1) McGrail, B. T.; Sehirlioglu, A.; Pentzer, E. Polymer Composites for Thermoelectric Applications. *Angew. Chem., Int. Ed.* **2015**, *54* (6), 1710−1723.

(2) Yusupov, K.; Vomiero, A. Polymer-Based Low-Temperature Thermoelectric Composites. *Adv. Funct. Mater.* **2020**, *30* (52), 2002015.

(3) Russ, B.; Glaudell, A. M.; Urban, J. J.; Chabinyc, M. L.; Segalman, R. A. Organic Thermoelectric Materials for Energy Harvesting and Temperature Control. *Nat. Rev. Mater.* **2016**, *1* (10), 16050.

(4) Li, G.; Zhu, R.; Yang, Y. Polymer Solar Cells. *Nat. Photonics* **2012**, *6* (3), 153−161.

(5) Jørgensen, M.; Norrman, K.; Gevorgyan, S. A.; Tromholt, T.; Andreasen, B.; Krebs, F. C. Stability of Polymer Solar Cells. *Adv. Mater.* **2012**, *24* (5), 580−612.

(6) Dou, L.; You, J.; Hong, Z.; Xu, Z.; Li, G.; Street, R. A.; Yang, Y. 25th Anniversary Article: A Decade of Organic/Polymeric Photovoltaic Research. *Adv. Mater.* **2013**, *25* (46), 6642−6671.

(7) Jacobs, I. E.; Moulé, A. J. Controlling Molecular Doping in Organic Semiconductors. *Adv. Mater.* **2017**, *29* (42), 1703063.

(8) Tang, S.; Irgum, K.; Edman, L. Chemical Stabilization of Doping in Conjugated Polymers. *Org. Electron.* **2010**, *11* (6), 1079−1087.

(9) Yamashita, Y.; Tsurumi, J.; Ohno, M.; Fujimoto, R.; Kumagai, S.; Kurosawa, T.; Okamoto, T.; Takeya, J.; Watanabe, S. Efficient Molecular Doping of Polymeric Semiconductors Driven by Anion Exchange. *Nature* **2019**, *572* (7771), 634−638.

(10) Jacobs, I. E.; Lin, Y.; Huang, Y.; Ren, X.; Simatos, D.; Chen, C.; Tjhe, D.; Statz, M.; Lai, L.; Finn, P. A.; et al. High-Efficiency Ion-Exchange Doping of Conducting Polymers. *Adv. Mater.* **2021**, *34* (22), 2102988.

(11) Murrey, T. L.; Riley, M. A.; Gonel, G.; Antonio, D. D.; Filardi, L.; Shevchenko, N.; Mascal, M.; Moulé, A. J. Anion Exchange Doping: Tuning Equilibrium to Increase Doping Efficiency in Semiconducting Polymers. *J. Phys. Chem. Lett.* **2021**, *12* (4), 1284−1289.

(12) Thomas, E. M.; Peterson, K. A.; Balzer, A. H.; Rawlings, D.; Stingelin, N.; Segalman, R. A.; Chabinyc, M. L. Effects of Counter-Ion Size on Delocalization of Carriers and Stability of Doped Semiconducting Polymers. *Adv. Electron. Mater.* **2020**, *6* (12), 2000595.

(13) Patel, S. N.; Glaudell, A. M.; Peterson, K. A.; Thomas, E. M.; O'Hara, K.; Lim, E.; Chabinyc, M. L. Morphology Controls the Thermoelectric Power Factor of a Doped Semiconducting Polymer. *Sci. Adv.* **2017**, *3* (6), 1700434.

(14) Aubry, T. J.; Winchell, K. J.; Salamat, C. Z.; Basile, V. M.; Lindemuth, J. R.; Stauber, J. M.; Axtell, J. C.; Kubena, R. M.; Phan, M. D.; Bird, M. J.; et al. Tunable Dopants with Intrinsic Counterion Separation Reveal the Effects of Electron Affinity on Dopant Intercalation and Free Carrier Production in Sequentially Doped Conjugated Polymer Films. *Adv. Funct. Mater.* **2020**, *30* (28), 2001800.

(15) Duong, Q. M.; Vidales, D. G.; Schwartz, B. J. The Effects of Humidity on the Electrical Properties and Carrier Mobility of Semiconducting Polymers Anion-Exchange Doped with Hygroscopic Salts. *Appl. Phys. Lett.* **2023**, *123* (20), 203301.

(16) Chai, H.; Xu, Z.; Li, H.; Zhong, F.; Bai, S.; Chen, L. Sequential-Twice-Doping Approach toward Synergistic Optimization of Carrier Concentration and Mobility in Thiophene-Based Polymers. *ACS Appl. Electron. Mater.* **2022**, *4* (10), 4947−4954.

(17) Thakur, R. M.; Easley, A. D.; Wang, S.; Zhang, Y.; Ober, C. K.; Lutkenhaus, J. L. Real Time Quantification of Mixed Ion and Electron Transfer Associated with the Doping of Poly(3-Hexylthiophene). *J. Mater. Chem. C* **2022**, *10* (18), 7251−7262.

(18) Yoon, S. E.; Park, J.; Kwon, J. E.; Lee, S. Y.; Han, J. M.; Go, C. Y.; Choi, S.; Kim, K. C.; Seo, H.; Kim, J. H.; et al. Improvement of Electrical Conductivity in Conjugated Polymers through Cascade Doping with Small-Molecular Dopants. *Adv. Mater.* **2020**, *32* (49), 2005129.
(19) Yuan, D.; Plunkett, E.; Nguyen, P. H.; Rawlings, D.; Le, M. L.; Kroon, R.; Müller, C.; Segalman, R. A.; Chabinyc, M. L. Double Doping of Semiconducting Polymers Using Ion-Exchange with a Dianion. *Adv. Funct. Mater.* **2023**, *33* (29), 2300934.
(20) Kim, T. H.; Kim, J. H.; Kang, K. Molecular Doping Principles in Organic Electronics: Fundamentals and Recent Progress. *Jpn. J. Appl. Phys.* **2023**, *62* (SE), SE0803.
(21) Filapek, M.; Hellwig, H.; Gancarz, P.; Szłapa-Kula, A. Influence of Various Doping Agents on Organic Semiconductors' Physicochemical Properties. *J. Electrochem. Soc.* **2021**, *168* (4), 046508.
(22) Krauss, G.; Hochgesang, A.; Mohanraj, J.; Thelakkat, M. Highly Efficient Doping of Conjugated Polymers Using Multielectron Acceptor Salts. *Macromol. Rapid Commun.* **2021**, *42* (22), 2100443.
(23) Salleo, A.; Kline, R. J.; DeLongchamp, D. M.; Chabinyc, M. L. Microstructural Characterization and Charge Transport in Thin Films of Conjugated Polymers. *Adv. Mater.* **2010**, *22* (34), 3812−3838.
(24) Wang, C.; Duong, D. T.; Vandewal, K.; Rivnay, J.; Salleo, A. Optical Measurement of Doping Efficiency in Poly(3-Hexylthiophene) Solutions and Thin Films. *Phys. Rev. B* **2015**, *91* (8), 085205.
(25) Duong, D. T.; Wang, C.; Antono, E.; Toney, M. F.; Salleo, A. The Chemical and Structural Origin of Efficient P-Type Doping in P3HT. *Org. Electron.* **2013**, *14* (5), 1330−1336.
(26) Ghosh, R.; Luscombe, C. K.; Hambsch, M.; Mannsfeld, S. C. B.; Salleo, A.; Spano, F. C. Anisotropic Polaron Delocalization in Conjugated Homopolymers and Donor−Acceptor Copolymers. *Chem. Mater.* **2019**, *31* (17), 7033−7045.
(27) Lu, G.; Blakesley, J.; Himmelberger, S.; Pingel, P.; Frisch, J.; Lieberwirth, I.; Salzmann, I.; Oehzelt, M.; Di Pietro, R.; Salleo, A.; et al. Moderate Doping Leads to High Performance of Semiconductor/Insulator Polymer Blend Transistors. *Nat. Commun.* **2013**, *4* (1), 1588.
(28) Yan, F.; Chen, R.; Sun, H. D.; Wei Sun, X. Silver Nanoparticle Facilitated Charge Generation in Tandem Organic Light-Emitting Devices. *Appl. Phys. Lett.* **2013**, *102* (20), 203304.
(29) Zhao, Y.; Opitz, A.; Eljarrat, A.; Kochovski, Z.; Koch, C. T.; Koch, N.; Lu, Y. Kinetic Study on the Adsorption of 2,3,5,6-Tetrafluoro-7,7,8,8-Tetracyanoquinodimethane on Ag Nanoparticles in Chloroform: Implications for the Charge Transfer Complex of Ag−F_4TCNQ. *ACS Appl. Nano Mater.* **2021**, *4* (11), 11625−11635.
(30) Guchait, S.; Dash, A.; Lemaire, A.; Herrmann, L.; Kemerink, M.; Brinkmann, M. Phase-Selective Doping of Oriented Regioregular Poly(3-Hexylthiophene-2,5-Diyl) Controls Stability of Thermoelectric Properties. *Adv. Funct. Mater.* **2024**, *34* (39), 2404411.
(31) Bredas, J. L.; Street, G. B. Polarons, Bipolarons, and Solitons in Conducting Polymers. *Acc. Chem. Res.* **1985**, *18* (10), 309−315.
(32) Voss, M. G.; Scholes, D. T.; Challa, J. R.; Schwartz, B. J. Ultrafast Transient Absorption Spectroscopy of Doped P3HT Films: Distinguishing Free and Trapped Polarons. *Faraday Discuss.* **2019**, *216*, 339−362.
(33) Beljonne, D.; Cornil, J.; Sirringhaus, H.; Brown, P. J.; Shkunov, M.; Friend, R. H.; Brédas, J. L. Optical Signature of Delocalized Polarons in Conjugated Polymers. *Adv. Funct. Mater.* **2001**, *11* (3), 229−234.
(34) Wu, E. C.-K.; Salamat, C. Z.; Tolbert, S. H.; Schwartz, B. J. Molecular Dynamics Study of the Thermodynamics of Integer Charge Transfer vs Charge-Transfer Complex Formation in Doped Conjugated Polymers. *ACS Appl. Mater. Interfaces* **2022**, *14* (23), 26988−27001.
(35) Barrett, B. J.; Saund, S. S.; Dziatko, R. A.; Clark-Winters, T. L.; Katz, H. E.; Bragg, A. E. Spectroscopic Studies of Charge-Transfer Character and Photoresponses of F_4TCNQ-Based Donor−Acceptor Complexes. *J. Phys. Chem. C* **2020**, *124* (17), 9191−9202.
(36) Arvind, M.; Tait, C. E.; Guerrini, M.; Krumland, J.; Valencia, A. M.; Cocchi, C.; Mansour, A. E.; Koch, N.; Barlow, S.; Marder, S. R.; et al. Quantitative Analysis of Doping-Induced Polarons and Charge-Transfer Complexes of Poly(3-Hexylthiophene) in Solution. *J. Phys. Chem. B* **2020**, *124* (35), 7694−7708.
(37) Stanfield, D. A.; Wu, Y.; Tolbert, S. H.; Schwartz, B. J. Controlling the Formation of Charge Transfer Complexes in Chemically Doped Semiconducting Polymers. *Chem. Mater.* **2021**, *33* (7), 2343−2356.
(38) Jacobs, I. E.; Cendra, C.; Harrelson, T. F.; Bedolla Valdez, Z. I.; Faller, R.; Salleo, A.; Moulé, A. J. Polymorphism Controls the Degree of Charge Transfer in a Molecularly Doped Semiconducting Polymer. *Mater. Horiz.* **2018**, *5* (4), 655−660.
(39) Kiefer, D.; Kroon, R.; Hofmann, A. I.; Sun, H.; Liu, X.; Giovannitti, A.; Stegerer, D.; Cano, A.; Hynynen, J.; Yu, L.; et al. Double Doping of Conjugated Polymers with Monomer Molecular Dopants. *Nat. Mater.* **2019**, *18* (2), 149−155.
(40) Ma, L.; Hu, P.; Jiang, H.; Kloc, C.; Sun, H.; Soci, C.; Voityuk, A. A.; Michel-Beyerle, M. E.; Gurzadyan, G. G. Single Photon Triggered Dianion Formation in TCNQ and F4TCNQ Crystals. *Sci. Rep.* **2016**, *6* (1), 28510.
(41) Neelamraju, B.; Watts, K. E.; Pemberton, J. E.; Ratcliff, E. L. Correlation of Coexistent Charge Transfer States in F4TCNQ-Doped P3HT with Microstructure. *J. Phys. Chem. Lett.* **2018**, *9* (23), 6871−6877.
(42) Watts, K. E.; Clary, K. E.; Lichtenberger, D. L.; Pemberton, J. E. FTIR Spectroelectrochemistry of F4TCNQ Reduction Products and Their Protonated Forms. *Anal. Chem.* **2020**, *92* (10), 7154−7161.
(43) Watts, K. E.; Neelamraju, B.; Moser, M.; McCulloch, I.; Ratcliff, E. L.; Pemberton, J. E. Thermally Induced Formation of HF_4TCNQ^- in F_4TCNQ-Doped Regioregular P3HT. *J. Phys. Chem. Lett.* **2020**, *11* (16), 6586−6592.
(44) Wu, E. C.; Schwartz, B. J. Does the Traditional Band Picture Describe the Electronic Structure of Doped Conjugated Polymers? TD-DFT and Natural Transition Orbital Study of Doped P3HT. *J. Chem. Theory Comput.* **2023**, *19* (19), 6761−6769.
(45) Wixtrom, A. I.; Shao, Y.; Jung, D.; Machan, C. W.; Kevork, S. N.; Qian, E. A.; Axtell, J. C.; Khan, S. I.; Kubiak, C. P.; Spokoyny, A. M. Rapid Synthesis of Redox-Active Dodecaborane $B_{12}(OR)_{12}$Clusters under Ambient Conditions. *Inorg. Chem. Front.* **2016**, *3* (5), 711−717.
(46) Aubry, T. J.; Axtell, J. C.; Basile, V. M.; Winchell, K. J.; Lindemuth, J. R.; Porter, T. M.; Liu, J.; Alexandrova, A. N.; Kubiak, C. P.; Tolbert, S. H.; et al. Dodecaborane-Based Dopants Designed to Shield Anion Electrostatics Lead to Increased Carrier Mobility in a Doped Conjugated Polymer. *Adv. Mater.* **2019**, *31* (11), 1805647.
(47) Panja, S.; Kadhane, U.; Andersen, J. U.; Holm, A. I. S.; Hvelplund, P.; Kirketerp, M.-B. S.; Nielsen, S. B.; Støchkel, K.; Compton, R. N.; Forster, J. S.; et al. Dianions of 7,7,8,8-Tetracyano-p-Quinodimethane and Perfluorinated Tetracyanoquinodimethane: Information on Excited States from Lifetime Measurements in an Electrostatic Storage Ring and Optical Absorption Spectroscopy. *J. Chem. Phys.* **2007**, *127* (12), 124308.
(48) Hobson, A. L.; Hussain, H.; Mousley, P. J.; Duncan, D. A.; Braim, M.; Costantini, G.; Nicklin, C.; Woodruff, D. P. Structure Determination of F_4TCNQ on Ag(111): A Systematic Trend in Metal Adatom Incorporation. *ACS Omega* **2024**, *9* (29), 32193−32200.
(49) Chae, I. S.; Kang, S. W.; Kang, Y. S. Olefin Separation via Charge Transfer and Dipole Formation at the Silver Nanoparticle−Tetracyanoquinoid Interface. *RSC Adv.* **2014**, *4* (57), 30156−30161.
(50) Wang, J.; Xu, W.; Zhang, J.; Xu, S. Ag Nanoparticles Decorated Small-Sized AgTCNQF_4Nanorod: Synthesis in Aqueous Solution and Its Photoinduced Charge Transfer Reactions. *J. Phys. Chem. C* **2014**, *118* (42), 24752−24760.
(51) Das, P.; Zayat, B.; Wei, Q.; Salamat, C. Z.; Magdău, I.-B.; Elizalde-Segovia, R.; Rawlings, D.; Lee, D.; Pace, G.; Irshad, A.; et al. Dihexyl-Substituted Poly(3,4-Propylenedioxythiophene) as a Dual Ionic and Electronic Conductive Cathode Binder for Lithium-Ion Batteries. *Chem. Mater.* **2020**, *32* (21), 9176−9189.
(52) Scholes, D. T.; Yee, P. Y.; McKeown, G. R.; Li, S.; Kang, H.; Lindemuth, J. R.; Xia, X.; King, S. C.; Seferos, D. S.; Tolbert, S. H.;

https://doi.org/10.1021/acs.jpcc.5c02950
J. Phys. Chem. C 2025, 129, 15771−15781

et al. Designing Conjugated Polymers for Molecular Doping: The Roles of Crystallinity, Swelling, and Conductivity in Sequentially-Doped Selenophene-Based Copolymers. *Chem. Mater.* **2019**, *31* (1), 73−82.
(53) Jacobs, I. E.; Aasen, E. W.; Oliveira, J. L.; Fonseca, T. N.; Roehling, J. D.; Li, J.; Zhang, G.; Augustine, M. P.; Mascal, M.; Moulé, A. J. Comparison of Solution-Mixed and Sequentially Processed P3HT:F4TCNQ Films: Effect of Doping-Induced Aggregation on Film Morphology. *J. Mater. Chem. C* **2016**, *4* (16), 3454−3466.
(54) Stanfield, D. A.; Mehmedović, Z.; Schwartz, B. J. Vibrational Stark Effect Mapping of Polaron Delocalization in Chemically Doped Conjugated Polymers. *Chem. Mater.* **2021**, *33* (21), 8489−8500.
(55) Duong, Q. M.; Garcia Vidales, D.; Salamat, C. Z.; Tolbert, S. H.; Schwartz, B. J. Measuring the Anisotropic Conductivity of Rub-Aligned Doped Semiconducting Polymer Films: The Role of Electrode Geometry. *Phys. Rev. Appl.* **2024**, *21*, 024006.

https://doi.org/10.1021/acs.jpcc.5c02950
J. Phys. Chem. C 2025, 129, 15771−15781